JOURNAL OF GUIDANCE, CONTROL, AND DYNAMICS
Vol. 23, No. 4, July–August 2000

Visual Aircraft Identification as a Pursuit–Evasion Game

Tuomas Raivio* and Harri Ehtamo†
Helsinki University of Technology, FIN-02015, Espoo, Finland

A new computational decomposition scheme is applied to a pursuit–evasion game that describes the visual identification of a foreign intruder aircraft in three dimensions. The intruder is assumed to minimize its distance to the state border at the time of identification, whereas the identifying aircraft wishes to intercept the intruder as far away inland as possible. The identification occurs when the identifier reaches the intruder's velocity and attitude within a given distance from it. The computational scheme decomposes the minimaximization of the payoff into two sequences of optimal control problems that can be solved using discretization and nonlinear programming techniques.

Introduction

IN this paper, we consider the final phase of an optimal visual identification of an intruding aircraft. The intruder is assumed to be a scout who has entered a state's air space and wishes to escape before being identified. The encounter is modeled as a pursuit–evasion game where the intruder corresponds to the evader and the identifying aircraft to the pursuer. Games where the evader wants to escape from a given area are sometimes referred to as life-line games (for example, see Ref. 1).

The study is motivated by the different goals and constraints compared to those aircraft pursuit–evasion problems in which the payoff is the final time and the terminal condition only involves the relative distance of the parties. Namely, it is not reasonable to assume that an intruder would aim at maximizing the capture time without considering the escape direction. From some initial constellations, a time optimal maneuver would require escaping inland. Moreover, a visual identification requires that the identifier achieves a similar attitude and velocity with the intruder in its vicinity. These requirements have been studied to some extent in the context of optimal control against a nonmaneuvering intruder,[2] but seemingly not in a game framework. For example, it is known that optimal solutions deviate from the solutions with a free final state and that the velocity adaptation requires deceleration. Because of the properties of the drag force of an aircraft, the deceleration can give rise to a chattering control arc (see Refs. 3 and 4). The game approach offers the additional possibility to simultaneously determine the optimal action of both parties against the worst action of the other one.

The game is solved using the decomposition method presented in Refs. 5 and 6. The minimaximization problem is decomposed into two subproblems that are solved anew at every iteration step. The subproblems are ordinary optimal control problems that can be solved efficiently by discretization and nonlinear programming techniques (see Refs. 3 and 7–9). The subproblems converge robustly because the convergence domain of direct approaches is substantially larger than that of indirect methods. Reasons for this are well known and sketched, for example in Ref. 10. Because of the direct approach, the necessary conditions are not explicitly involved in the solution process. This is a remarkable benefit, because with complicated game dynamics the necessary conditions can be difficult to solve numerically. In Refs. 5 and 6 the convergence of the method is analyzed, and it is shown that in the case of convergence the solution satisfies the regular necessary conditions of an open-loop representation[11] of a saddle point in feedback strategies. The studied numerical examples show that the method offers an efficient tool for rapid solution of complex pursuit–evasion games.

Received 28 May 1999; revision received 20 December 1999; accepted for publication 22 December 1999.

*Assistant Professor, Systems Analysis Laboratory, P.O. Box 1100; tuomas.raivio@hut.fi.

†Professor, Systems Analysis Laboratory; harri.ehtamo@hut.fi.

In the following paper, the identification procedure and the aircraft models are first described. The possibility of chattering control arcs is ruled out by convexifying the players' sets of admissible state rates. Normally the solution of the convexified problem only represents the limiting case of a chattering control arc, but here the convexification can be interpreted as constrained use of a wing air brake. The corresponding pursuit–evasion game model is then set up and the solution method is described briefly. Finally, the method is applied to produce numerical open-loop representations of feedback saddle point trajectories from some initial constellations.

Visual Identification Procedure and Aircraft Models

When an intruding aircraft violates the air space of a state, a visual identification procedure is initiated. One or more aircraft are deployed to perform the identification and to inform the intruder of the violation. A visual identification requires that the identifying aircraft achieves almost the same flight direction and velocity as the intruder within a relatively small distance behind it.

Three main scenarios on the intentions of the intruder are possible. First, the intruder might attack, which leads to an air combat between the intruder and the identifiers. Second, the intruder can be a lost aircraft that will act cooperatively and will not try to hinder the identification. Third, the intruder can be a scout whose objective is simply to avoid identification. We will concentrate on the optimal visual identification by a single aircraft P against a scout intruder E, who tries to escape before becoming identified.

Assuming that the initial distance between the parties is large, a good approximation of P's optimal trajectory is obtained by dividing the flight into a time optimal climb to the highest possible velocity and the respective altitude, a steady cruise in this altitude toward the expected rendezvous point, and a final transient to match the flight state with E (see, for example, Ref. 12). Here we consider the final phase that is assumed to begin as soon as the intruder E commences its evasion and terminates on identification.

Both P and E maneuver in three dimensions. With slight simplifications (see Ref. 13) and quadratic drag polar assumption, the dynamics of the parties are described by the following system of differential equations:

$$\dot{x}_i = v_i \cos\gamma_i \cos\chi_i \tag{1}$$

$$\dot{y}_i = v_i \cos\gamma_i \sin\chi_i \tag{2}$$

$$\dot{h}_i = v_i \sin\gamma_i \tag{3}$$

$$\dot{\gamma}_i = (g/v_i)(n_i \cos\mu_i - \cos\gamma_i) \tag{4}$$

$$\dot{\chi}_i = \frac{g}{v_i}\frac{n_i \sin\mu_i}{\cos\gamma_i} \tag{5}$$

$$\begin{aligned}\dot{v}_i = (1/m_i)\big\{&u_i T_{\max,i}[h_i, M(h_i, v_i)] \\ &- D_{0,i}[h_i, v_i, M(h_i, v_i)] - n_i^2 D_{I,i}[h_i, v_i, M(h_i, v_i)] \\ &- D_{br,i}[h_i, v_i, M(h_i, v_i), \eta_i]\big\} - g\sin\gamma_i, \qquad i = P, E\end{aligned} \tag{6}$$

The state variables x, y, h, v, γ, and χ describe the positions, velocities, flight-path angles, and the heading angles of both aircraft in three dimensions, respectively. The heading angle is measured counterclockwise from the positive x axis. The aircraft are controlled by the throttle settings u_P and u_E, the loadfactors n_P and n_E, and the bank angles μ_P and μ_E. In addition, both aircraft are equipped with a wing air brake. The wing air brakes are controlled by their opening angles η_P and η_E. The gravitational acceleration g, as well as the masses m_P and m_E of the aircraft are assumed constant. The Mach number is denoted by $M(h, v)$, or, briefly, M.

For both players, the zero-lift drag $D_{0,i}(\cdot)$ and induced drag $D_{I,i}(\cdot)$ are described by

$$D_{0,i} = C_{D_0,i}(M_i) S_i q(h_i, v_i) \tag{7}$$

$$D_{I,i} = K_i(M_i) \frac{(m_i g)^2}{S_i q(h_i, v_i)}, \qquad i = P, E \tag{8}$$

where $C_{D_0,i}(M)$ and $K_i(M)$ denote the zero-lift and induced drag coefficients, respectively. The reference wing areas of the aircraft are denoted by S and the dynamic pressure by $q(h, v) = 1/2\varrho(h)v^2$. The air density $\varrho(h)$ and the Mach number are computed using the International Standard Atmosphere. The incremental drag due to the wing air brakes is of the form

$$D_{br,i}(h_i, v_i, M_i, \eta_i) = C_{D,br,i}(M_i, \eta_i) S_i q(h_i, v_i), \qquad i = P, E \tag{9}$$

where $C_{D,br,i}(M_i, \eta_i)$, $i = P, E$, are the airbrake drag coefficients of the players. The coefficients $C_{D_0,i}(M)$ and $K_i(M)$, $i = P, E$, are approximated for both players by rational polynomials on the basis of realistic tabular data. The maximal thrust forces $T_{\max,i}(h_i, M_i)$, $i = P, E$, are approximated with two dimensional polynomials. A similar approach could be taken with the airbrake drag coefficients, but it turns out to be unnecessary, as will be shown. The parameters of the players resemble two modern high-performance fighter aircraft.

The following box constraints are imposed on the controls:

$$n_i \in [n_{\min}, n_{\max}] = [0, 9] \tag{10}$$

$$\mu_i \in [-\pi, \pi[\tag{11}$$

$$u_i \in [0, 1], \qquad i = P, E \tag{12}$$

The opening angles η_P and η_E are constrained by

$$0 \le \eta_i \le \eta_{\max,i}(h_i, M_i), \qquad i = P, E \tag{13}$$

The upper limit is imposed to avoid actuator damages.

Both aircraft have to stay in their flight envelopes. In the present model the boundaries of interest are the minimum altitude constraints

$$h_P, h_E \ge h_{\min} \tag{14}$$

and the dynamic pressure constraints

$$q(h_P, v_P) \le q_{P,\max} \tag{15}$$

$$q(h_E, v_E) \le q_{E,\max} \tag{16}$$

We set $q_{P,\max} > q_{E,\max}$ to guarantee the termination of the game.

Modification of the Players' Hodographs

The set of admissible state rates of a dynamic system at a given state is sometimes called the hodograph (see, for example, Ref. 3 and references cited therein). The hodograph of the aircraft models described is nonconvex because of the induced drag term in Eq. (6). According to the model, the aircraft achieves a larger deceleration rate by selecting $u = 0$ and $n = n_{\max}$ than just by selecting $u = 0$. Nevertheless, selecting $n = n_{\max}$ will not necessarily drive the aircraft to the given terminal conditions. Therefore, if rapid velocity dissipations are required, a chattering control arc arises. That is, $u^* = 0$, $n^* = n_{\max}$, and the bank angle switches rapidly between two values that are π rad apart. In the limit the rate is infinite, and neither the heading angle nor the flight path angle are affected. Of course, this kind of control function is unadmissible and cannot be realized in practice.

If the players are anticipated to decelerate at the end of the identification, the aircraft model introduced in the preceding section is inappropriate as such. In optimal control framework, one way to guarantee the existence of the solution is to convexify the hodograph. This means that the model is altered such that the hodograph is replaced by its convex hull. The solution then represents the limit case of a chattering control solution with a somewhat imprecise interpretation.

Here we clarify the meaning of the convexification by replacing the wing air brake opening angle constraint (13) by the following loadfactor-dependent constraint:

$$0 \le D_{br,i}(h_i, v_i, M_i, \eta_i) \le n_{\max}^2 D_{I,i}(h_i, v_i, M_i) - n_i^2 D_{I,i}(h_i, v_i, M_i), \qquad i = P, E \tag{17}$$

The constraint allows full use of the wing air brake at $n = 0$ but completely prevents the use at $n = n_{\max}$. At $u = 0$, the largest possible deceleration can now be selected using η only, and the resulting hodographs of the players are convex.

The use of the constraint (17) would require two-dimensional approximation of $C_{D,br}(M, \eta)$ from tabular data for both P and E. We therefore follow the approach outlined in Ref. 12. The throttle settings and the opening angles are aggregated into single control variables δ_P and δ_E, Eq. (6) is replaced with

$$\dot{v}_i = (1/m_i)\left\{\delta_i\left[T_{\max,i}(h_i, M_i) - \left(n_i^2 - n_{\max}^2\right) D_{I,i}(h_i, v_i, M_i)\right] - D_{0,i}(h_i, v_i, M_i) - n_{\max}^2 D_{I,i}(h_i, v_i, M_i)\right\} - g \sin\gamma_i \qquad i = P, E \tag{18}$$

and constraints (12) and (13) are replaced with

$$\delta_i \in [0, 1], \qquad i = P, E \tag{19}$$

For both P and E, constraints (10) and (17) and Eq. (6) are equivalent to constraint (19) and Eq. (18) in the sense that they yield the same admissible velocity rates. In other words, the convexified hodograph does not change. If desired, the original control variable histories for both P and E can be computed afterward using the state variable histories, $D_{br,P}(h_P, v_P, M_P, \eta_P)$, and $D_{br,E}(h_E, v_E, M_E, \eta_E)$.

When giving the preceding interpretation for the convexification, we are assuming that the wing air brakes of the players can produce the required drag difference. For the considered aircraft models, this assumption seems to hold in altitudes below 5000 m and velocities larger than 300 m/s. Even if the assumption does not hold, the results still have some significance as the limiting solutions of a chattering control.

Pursuit–Evasion Game

We assume that the players have perfect information on the state of the game, which is described by the state vector

$$z = [z_P', z_E']' = [x_P, y_P, h_P, v_P, \gamma_P, \chi_P, x_E, y_E, h_E, v_E, \gamma_E, \chi_E]' \tag{20}$$

where the prime denotes a transpose. The control vectors of the players are $\tilde{u}_P = [n_P, \mu_P, \delta_P]'$ and $\tilde{u}_E = [n_E, \mu_E, \delta_E]'$. They are restricted by the constraints (10), (11), and (19). The evolution of the state is described by Eqs. (1–5) and (18), and the state space is restricted by the constraints (14–16).

The engagement is assumed to begin as soon as the evader, once having noticed the pursuer, commences an evasive maneuver. The initial conditions are given as

$$[z_P'(0), z_E'(0)]' = [z_{P0}', z_{E0}']' = z_0 \tag{21}$$

and the game terminates as soon as the capture condition

$$l[z_P(T), z_E(T)] = [x_P(T) - x_E(T)]^2 + [y_P(T) - y_E(T)]^2 + [h_P(T) - h_E(T)]^2 + \kappa[v_P(T) - v_E(T)]^2 + \xi[\gamma_P(T) - \gamma_E(T)]^2 + \iota[\chi_P(T) - \chi_E(T)]^2 - d^2 = 0 \tag{22}$$

becomes satisfied. The weights κ, ξ, and ι are introduced to scale the values of the terms into the same magnitude. The parameter d represents the capture radius, a measure for the difference in position and flight state. The capture condition determines the final time T. We assume that the pursuer's optimal trajectories terminate behind the evader. For short initial separations and large initial velocity differences, numerical solution methods may yield trajectory pairs where the pursuer ends up in a point that satisfies the capture condition but lies in front of the evader. Therefore, the assumption has to be verified afterward.

The objective of a scout intruder is to leave the foreign air state before being identified. We define the payoff of the game as the opposite of the evader's minimum distance to the state border at the time of capture,

$$J[\tilde{\boldsymbol{u}}_P, \tilde{\boldsymbol{u}}_E] = \tilde{p}[z_P(T), z_E(T)] := -\min_{\tau} \|[x_E(T), y_E(T)]' - [x_B(\tau), y_B(\tau)]'\|_2 \tag{23}$$

where $[x_B(\tau), y_B(\tau)]'$ is some parameterized representation of the border. At this stage we approximate the border by a straight line $x_B(\tau) = c$, $y_B(\tau)$ free. Hence, the payoff can be expressed in a much simpler form,

$$J[\tilde{\boldsymbol{u}}_P, \tilde{\boldsymbol{u}}_E] = p[z_P(T), z_E(T)] := x_E(T) \tag{24}$$

The evader now strives for maximizing his final x coordinate, whereas the pursuer aims at minimizing it. Both maximization and minimization take place subject to the state equation and the control as well as state variable inequality constraints described earlier.

A capture is possible from any initial state if we assume that the pursuer is faster and more agile than the evader.[14] However, what distinguishes a successful identification from an unsuccessful one is the value of the game. If $x_E^*(T) < c$, where the asterisk denotes the saddle point solution, the capture takes place before the border is reached and the identification is successful. Otherwise the identification is considered unsuccessful.

Solution Method

The described pursuit–evasion game is a complex one and certainly cannot be solved analytically. An open-loop representation of a feedback saddle point solution, corresponding to a given initial state, can be computed by solving the corresponding necessary conditions. Near optimal feedback solutions can then be synthesized on the basis of a cluster of open-loop representations related to different initial states. The necessary conditions form a high-dimensional multipoint boundary value problem with a free boundary and an unknown amount of adjoint equation discontinuities and corners at unknown times. Furthermore, the payoff of the game does not allow a state-space reduction with respect to the x coordinates of the players. The boundary value problem could be solved using, for example, multiple shooting (see Ref. 15) or some other appropriate method. This indirect approach provides detailed results but has some drawbacks, the most severe perhaps being the need for a precise initial estimate of the solution to achieve convergence.

For games in which the state equation and the control, as well as the state variable inequality constraints, are separable with respect to the players' control and state variables, and the payoff is terminal, the necessary conditions are coupled only at $t = T$ through the payoff and the terminal manifold. Clearly, the game under consideration belongs to this category. In Ref. 5 we present a method that decomposes the solution of the necessary conditions of such games into two separate subproblems that are solved iteratively. The subproblems are optimal control problems, and at the end of the iteration, the necessary optimality conditions of these problems coincide with the necessary conditions of the game.

The motivation of the decomposition is that the subproblems can be solved using not only indirect methods but also discretization and nonlinear programming approaches, which in many respects have benefits compared to the indirect methods. For a comprehensive summary see, for example, Ref. 10. The necessary conditions are then not directly involved in the solution process, but the solution approximately satisfies them. Optimal decision variables of the discretized problems approximate the optimal continuous-time state and control histories, and the Lagrange multipliers approximate the adjoint trajectories. Of course, indirect methods could be used in solving the subproblems as well.

We now explain the decomposition method in more detail. If we assume that the minimum and the maximum operators commute, the maxmin solution of a pursuit–evasion game will coincide with the minmax and the saddle point solution. Then, an open-loop representation of the feedback saddle point solution can be computed by solving the maxmin problem, defined by

$$\max_{\tilde{\boldsymbol{u}}_E} \min_{\tilde{\boldsymbol{u}}_P} p[z_P(T), z_E(T)] \tag{25}$$

$$\dot{z}_i(t) = \boldsymbol{f}_i[z_i(t), \tilde{\boldsymbol{u}}_i(t)], \qquad z_i(0) = z_{i0} \tag{26}$$

$$\boldsymbol{C}_i[z_i(t), \tilde{\boldsymbol{u}}_i(t)] \le \boldsymbol{0} \tag{27}$$

$$\boldsymbol{S}_i[z_i(t)] \le \boldsymbol{0}, \qquad i = P, E \tag{28}$$

$$l[z_P(T), z_E(T)] = 0 \tag{29}$$

where Eqs. (27) and (28) describe the control and the path constraints that here consist of Eqs. (10), (11), (14–16), and (19). To obtain the maxmin solution we adopt the following iterative process. At each iteration, the pursuer's minimization problem is first solved while the current trajectory of the evader is kept fixed. The evader's trajectory is then corrected by a feasible improving step. To begin with, consider the minimization problem, given by

$$\min_{\tilde{\boldsymbol{u}}_P, T} p\left[z_P(T), z_E^0(T)\right] \tag{30}$$

$$\dot{z}_P(t) = \boldsymbol{f}_P[z_P(t), \tilde{\boldsymbol{u}}_P(t)], \qquad z_P(0) = z_{P0} \tag{31}$$

$$\boldsymbol{C}_P[z_P(t), \tilde{\boldsymbol{u}}_P(t)] \le \boldsymbol{0} \tag{32}$$

$$\boldsymbol{S}_P[z_P(t)] \le \boldsymbol{0} \tag{33}$$

$$l\left[z_P(T), z_E^0(T)\right] = 0 \tag{34}$$

where $z_E^0(t)$, $t \ge 0$, is a feasible nominal trajectory of the evader. Let the pursuer's solution trajectory be $\bar{z}_P(t)$ and the final time $\bar{T}$ and denote the capture point $z_E^0(\bar{T})$ by $\bar{\boldsymbol{e}}$. Now, $\bar{z}_P(t)$ is also an optimal trajectory for the problem where the evader's trajectory is replaced by the fixed point $\bar{\boldsymbol{e}}$ and the final time is fixed to $\bar{T}$. In the neighborhood of $(\bar{\boldsymbol{e}}, \bar{T})$, define the pursuer's value function, corresponding to a given initial state $z_{P,0}$ as a function of the capture point $(\boldsymbol{e}, T)$ by

$$\tilde{V}(\boldsymbol{e}, T) = \min_{\tilde{\boldsymbol{u}}_P} \{p[z_P(T), \boldsymbol{e}] \mid \dot{z}_P(t) = \boldsymbol{f}_P[z_P(t), \tilde{\boldsymbol{u}}_P(t)], \; t \in [0, T], z_P(0) = z_{P0}, \boldsymbol{C}_P[z_P(t), \tilde{\boldsymbol{u}}_P(t)] \le 0, \; \boldsymbol{S}_P[z_P(t)] \le \boldsymbol{0}, l[z_P(T), \boldsymbol{e}] = 0\} \tag{35}$$

Thus,

$$\tilde{V}(\bar{\boldsymbol{e}}, \bar{T}) = p[\bar{z}_P(\bar{T}), \bar{\boldsymbol{e}}] \tag{36}$$

The evader's problem is to maximize $\tilde{V}(\boldsymbol{e}, T)$ subject to the evader's constraints. Hence, the original maxmin problem (25–29) can be written as

$$\max_{\tilde{\boldsymbol{u}}_E, T} \tilde{V}[z_E(T), T] \tag{37}$$

$$\dot{z}_E(t) = \boldsymbol{f}_E[z_E(t), \tilde{\boldsymbol{u}}_E(t)], \qquad z_E(0) = z_{E0} \tag{38}$$

$$\boldsymbol{C}_E[z_E(t), \tilde{\boldsymbol{u}}_E(t)] \le \boldsymbol{0} \tag{39}$$

$$\boldsymbol{S}_E[z_E(t)] \le \boldsymbol{0} \tag{40}$$

This problem is difficult to solve as such, because $\tilde{V}(\cdot)$ cannot be expressed analytically. Therefore, we approximate the solution of the problem by the solution of the linearized problem where the final time is fixed to $\bar{T}$ and $\tilde{V}(\boldsymbol{e}, \bar{T})$ is replaced by its linear approximation. The approximation is given by

$$\tilde{V}(\bar{\boldsymbol{e}}, \bar{T}) + \frac{\partial}{\partial \boldsymbol{e}} \tilde{V}'(\bar{\boldsymbol{e}}, \bar{T})(\boldsymbol{e} - \bar{\boldsymbol{e}}) \tag{41}$$

Basic sensitivity results (see Ref. 5 and the references cited therein) imply that the gradient of $\tilde{V}(\boldsymbol{e}, T)$ with respect to $\boldsymbol{e}$ at $(\bar{\boldsymbol{e}}, \bar{T})$ is given by the analytical expression

$$\frac{\partial}{\partial \boldsymbol{e}} \tilde{V}(\bar{\boldsymbol{e}}, \bar{T}) = \frac{\partial}{\partial \boldsymbol{e}} p[\bar{\boldsymbol{z}}_P(\bar{T}), \bar{\boldsymbol{e}}] + \bar{\alpha} \frac{\partial}{\partial \boldsymbol{e}} l[\bar{\boldsymbol{z}}_P(\bar{T}), \bar{\boldsymbol{e}}] \tag{42}$$

where $\bar{\alpha}$ is the Lagrange multiplier associated with the capture condition (34) in the solution of the problem [see Eqs. (30–34)]. The feasible improving step is now taken by solving the linearized problem that can be written as follows (recall that the first term of Eq. (41) is constant):

$$\max_{\tilde{\boldsymbol{u}}_E} \frac{\partial}{\partial \boldsymbol{e}} \tilde{V}(\bar{\boldsymbol{e}}, \bar{T})'[\boldsymbol{z}_E(\bar{T}) - \bar{\boldsymbol{e}}] \tag{43}$$

$$\dot{\boldsymbol{z}}_E(t) = \boldsymbol{f}_E[\boldsymbol{z}_E(t), \tilde{\boldsymbol{u}}_E(t)], \qquad t \in [0, T], \quad \boldsymbol{z}_E(0) = \boldsymbol{z}_{E0} \tag{44}$$

$$\boldsymbol{C}_E[\boldsymbol{z}_E(t), \tilde{\boldsymbol{u}}_E(t)] \leq \boldsymbol{0} \tag{45}$$

$$\boldsymbol{S}_E[\boldsymbol{z}_E(t)] \leq \boldsymbol{0} \tag{46}$$

Denote the solution trajectory of the problem (43–46) by $\boldsymbol{z}_E^1(t)$. Also denote $T^1 = \bar{T}$. One iteration is completed by extending $\boldsymbol{z}_E^1(t)$ for $t > T^1$, for example, linearly by

$$\boldsymbol{z}_E^1(t) = \begin{cases} \boldsymbol{z}_E^1(t), & t \leq T^1 \\ \boldsymbol{z}_E^1(T^1) + \dot{\boldsymbol{z}}_E^1(T^1)(t - T^1), & t > T^1 \end{cases} \tag{47}$$

The extended solution is then substituted back to the minimization problem (30–34) that is solved anew to locate the new capture point and to evaluate the linear approximation of $\tilde{V}(\cdot)$ at that point. The extension is needed because if convergence has not yet been achieved, the next $\bar{T}$ can be larger than T^1. The iteration is then continued by solving problems (43–46) and (30–34) by turns, until the relative change of $\tilde{V}(\cdot)$ becomes smaller than the desired relative accuracy.

In Ref. 5 it is shown that if convergence is achieved, the necessary optimality conditions of the optimal control problems coincide with the necessary conditions of the saddle point solution of the original game problem, under the given assumption that the maxmin solution coincides with the saddle point solution. In some cases this assumption may fail. For example, the saddle point solution can contain certain singular surfaces, peculiar to pursuit–evasion games only, that do not have a counterpart in the calculus of variations.[14] These surfaces require additional necessary conditions to be satisfied that cannot be expressed as optimality conditions of the subproblems of the described solution method. The surfaces include at least the equivocal surface (see Refs. 11 and 14). To date, there does not exist any systematical method to detect these surfaces, and they have to be analyzed separately.[11] In the computations of this paper we assume that none of the mentioned surfaces appear. Should this happen, one obtains a maxmin solution that in practice may also be of interest.

On the other hand, when discretization and nonlinear programming are used in solving the subproblems, the singular surfaces appearing in them are automatically detected. The correct sequence of the unconstrained, constrained, and singular solution arcs of the subproblems needs not be specified in advance because, the necessary conditions are not directly involved in the solution process. For example, the activation of the dynamic pressure constraints (15) and (16) and the likely related singular control arcs will automatically become roughly approximated.

In the aforementioned approach, the saddle point problem is first decomposed and the subproblems are then discretized. In Ref. 6, we present an analysis where the game problem itself is parameterized at the outset by discretizing the players' dynamics. The parameterized problem is actually a special case of a bilevel programming problem (see, for example, Ref. 16), where the maximization is identified with the upper level problem and the minimization with the lower level problem. Reference 6 shows that in this framework, the presented decomposition method can be interpreted as a feasible direction method that under standard assumptions converges to a point satisfying the necessary conditions.

Numerical Solutions

In this section we solve the game numerically from some representative initial states. The optimal control problems appearing in the decomposition method above are discretized using direct transcription and the approach presented in Ref. 7. In this approach, the time history is divided into segments by a suitable discretization grid. The control and the state variables are assumed to be known only at the gridpoints. On each segment, the control trajectories are approximated linearly and the state trajectories with a cubic polynomial. Both approximations are required to be continuous and the cubics also smooth on their first derivative across the gridpoints. In the middle of each segment, the slope of the cubic is required to coincide with the system time rate of change. The control and the state variables at the gridpoints are selected such that these constraints hold, the control and state variable constraints are satisfied, and the object function of the problem is minimized or maximized.

An equidistant discretization grid with 25 discretization points is used. The number of points is considered sufficient because the payoffs and the solutions of the presented examples do not change considerably when denser grids are used. A more sophisticated approach would be to use nonequidistant grids where the number and the distribution of the gridpoints are controlled adaptively, for example, by monitoring and comparing the derivatives of the cubics and the state equations. Here, the equidistant grid is employed for the sake of simplicity.

The resulting nonlinear programming problems are solved using NPSOL,[17] which is a versatile implementation of the sequential quadratic programming (SQP) method. In SQP, at each iteration a quadratic programming problem consisting of a quadratic approximation of the objective function and a linear approximation of the constraints at the current point is solved, and a line search is carried out in the direction of the solution. In NPSOL, the use of an augmented Lagrangian merit function in the line search further enhances the convergence.

The iteration is executed until the relative change of $\tilde{V}(\boldsymbol{e}, T)$ becomes less than 0.1%. At this point, also the relative changes of the capture point and final time are of the same order. In every example, $q_{P,\max}$ and $q_{E,\max}$ in Eqs. (15) and (16) are set to 120 and 80 kPa, respectively. The pursuer's limit is selected quite large to guarantee termination in reasonable time. The minimum altitude is set to 50 m for both parties.

In the present game model, the gradient (42) at iteration k is given by

$$\begin{aligned} \frac{\partial}{\partial \boldsymbol{e}} \tilde{V}(\bar{\boldsymbol{e}}, \bar{T}) = \Big\{ & 1 - 2\bar{\alpha}\big[\bar{x}_P(\bar{T}) - x_E^k(\bar{T})\big], -2\bar{\alpha}\big[\bar{y}_P(\bar{T}) - y_E^k(\bar{T})\big], \\ & -2\bar{\alpha}\big[\bar{h}_P(\bar{T}) - h_E^k(\bar{T})\big], -2\bar{\alpha}\kappa\big[\bar{v}_P(\bar{T}) - v_E^k(\bar{T})\big], \\ & -2\bar{\alpha}\xi\big[\bar{\gamma}_P(\bar{T}) - \gamma_E^k(\bar{T})\big], -2\bar{\alpha}\iota\big[\bar{\chi}_P(\bar{T}) - \chi_E^k(\bar{T})\big] \Big\}' \end{aligned} \tag{48}$$

In the computation we use $d = 200$, $\kappa = 50$, and $\xi = \iota = 1000$.

Example 1: Intruder Approaching from the Border

First, consider a scenario where a subsonic evader approaches initially from the east and flies to the west, perpendicularly to the borderline. The pursuer approaches the evader from the south, see Fig. 1a. We assume that the pursuer has had the time to climb to an optimal cruise altitude and maximal velocity at that altitude. The engagement is assumed to begin as the horizontal separation of the parties is reduced to 10 km. A representative initial state z_0 corresponding to this engagement is

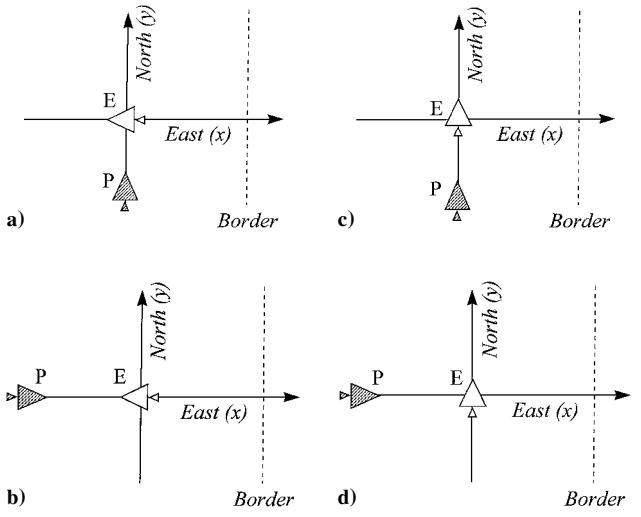

Fig. 1 Schematic view of the initial states under consideration; intruder or evader is white and identifier or pursuer shaded.

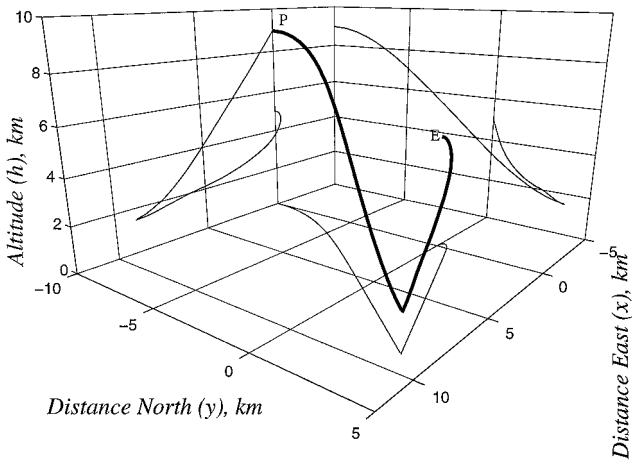

Fig. 2 Solution trajectories of the players and their projections in the *xy*, *xh*, and *yh* planes in the first case of example 1.

$$x_{P,0} = 0 \text{ m}, \qquad x_{E,0} = 0 \text{ m}$$

$$y_{P,0} = -10{,}000 \text{ m}, \qquad y_{E,0} = 0 \text{ m}$$

$$h_{P,0} = 9000 \text{ m}, \qquad h_{E,0} = 5000 \text{ m}$$

$$v_{P,0} = 550 \text{ m/s} = \text{Mach } 1.8, \qquad v_{E,0} = 200 \text{ m/s} = \text{Mach } 0.6$$

$$\gamma_{P,0} = 0 \text{ rad}, \qquad \gamma_{E,0} = 0 \text{ rad}$$

$$\chi_{P,0} = \pi/2 \text{ rad}, \qquad \chi_{E,0} = \pi \text{ rad}$$

The optimal trajectories of both players, together with projections on the coordinate planes, are presented in Fig. 2. Optimal control variable and velocity histories are presented in Fig. 3. The evader turns to the east almost in the vertical plane by diving steeply. The dive is soon constrained by the dynamic pressure limit that makes the evader reduce the thrust (see Figs. 3a, 3c, and 4). The optimal direction of return is not perpendicular to the border because the evader can delay the identification by moving also northward. The pursuer turns toward the expected rendezvous point and descends to match the altitude with that of the evader. Note that unlike in many games where the payoff is the final time, the players do not end up in a common vertical plane, cf. Ref. 18.

The requirement for equal velocities forces the pursuer to switch off the throttle and use the airbrake before the capture (see Fig. 3c). The relatively large velocity during the braking ensures that the wing air brake would indeed be able to produce the assumed deceleration.

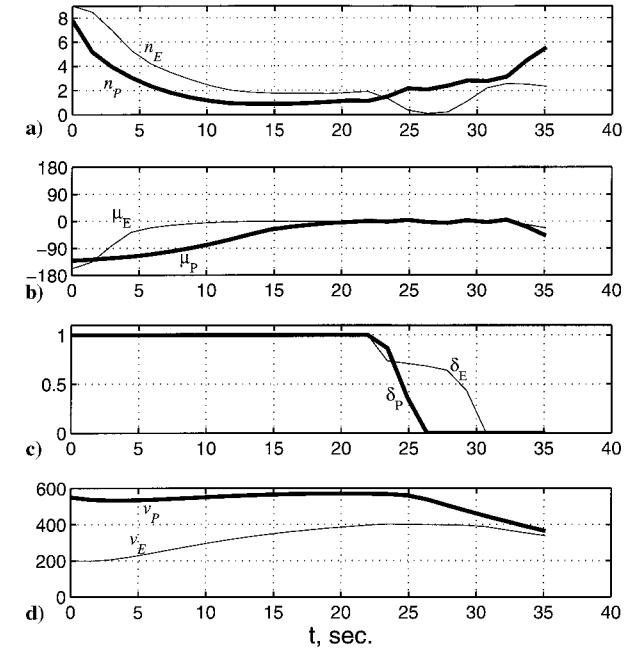

Fig. 3 In the first case of example 1: a) loadfactors, b) bank angles (deg), c) aggregated controls δ_P and δ_E, and d) velocities (m/s).

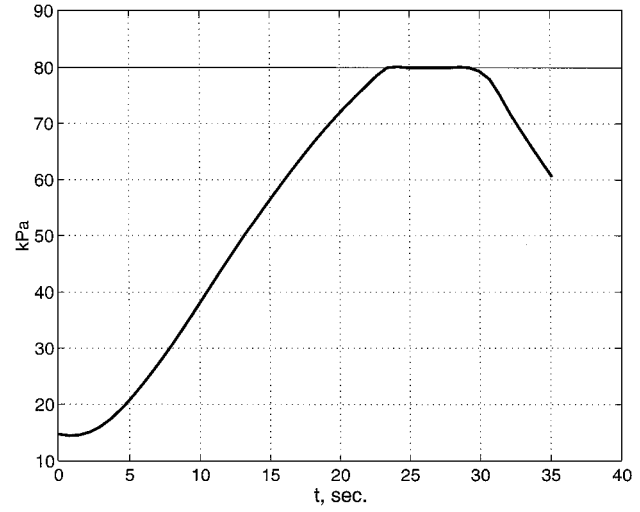

Fig. 4 Dynamic pressure of the evader in the first case of example 1.

An inspection shows that the pursuer stays behind the evader during the whole engagement.

There appears an interesting feature in this solution and the other solutions as well. Namely, in the end of the game the evader leaves the dynamic pressure constraint and decelerates as well (see Figs. 3c, 3d, and 4). By decelerating the evader loses velocity but also delays the capture, and the net effect of the deceleration on the payoff is positive. Also the evader's velocity during the braking is sufficient for the airbrake. Note the final transient in the bank angles of the players in Fig. 3b, too. As relatively large value of ι is used, the pursuer needs to adjust its heading angle, and the evader can again gain by reacting to this adjustment. Overall, the evader is able to move 8.97 km eastward before the capture. The engagement lasts 35.1 s.

One could speculate that there exists another solution associated with this initial state, in which the evader would turn to its left, toward the pursuer. The pursuer should then either perform a hard turn or even a loop to satisfy the final state constraints. This example, however, and other examples corresponding to different initial separations, altitude differences, and pursuer's velocities ensure that turning left leads to a local maxmin solution with a smaller payoff than in the saddle point solution. The pursuer is agile enough to capture the evader much earlier than when the evader turns right. Only

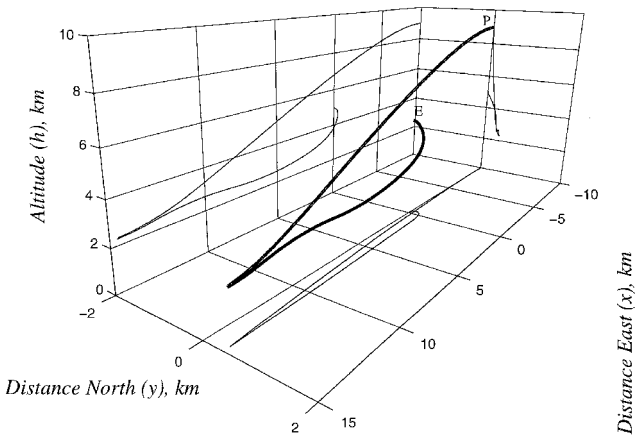

Fig. 5 Saddle point trajectories of the players in the second case of example 1.

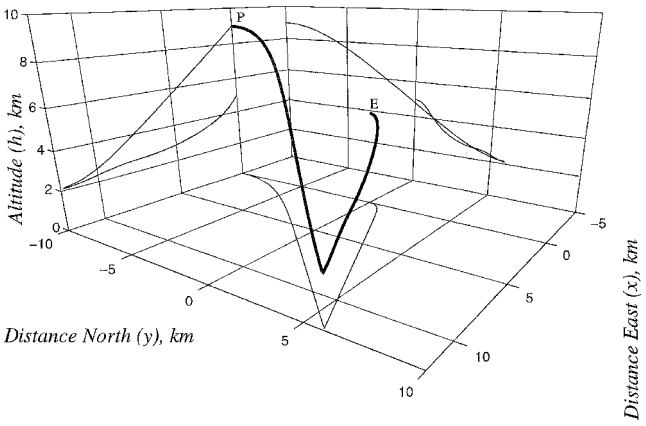

Fig. 6 Saddle point trajectories of the players in the first case of example 2.

in some rather unlikely scenarios where the pursuer lies initially very close to the evader and has a small initial velocity, turning left would be the correct solution. On the other hand, in modeling the encounter, the evader was tacitly assumed to behave in a nonaggressive way that does not include a head-on challenge.

It may happen that the pursuer is forced to approach the evader initially from the front. The solution trajectories corresponding to the initial state (see Fig. 1b)

$$\begin{aligned} x_{P,0} &= -10{,}000\ \text{m}, & x_{E,0} &= 0\ \text{m} \\ y_{P,0} &= 0\ \text{m}, & y_{E,0} &= 0\ \text{m} \\ h_{P,0} &= 9000\ \text{m}, & h_{E,0} &= 5000\ \text{m} \\ v_{P,0} &= 550\ \text{m/s} = \text{Mach } 1.8, & v_{E,0} &= 200\ \text{m/s} = \text{Mach } 0.6 \\ \gamma_{P,0} &= 0\ \text{rad}, & \gamma_{E,0} &= 0\ \text{rad} \\ \chi_{P,0} &= 0\ \text{rad}, & \chi_{E,0} &= \pi\ \text{rad} \end{aligned}$$

are presented in Fig. 5. The initial state lies actually on a dispersal surface of the evader (see Ref. 14) who must instantaneously decide whether to turn left or right. In this constellation, approaching from the front is less advantageous than approaching from the side, as the evader can now move 14.8 km eastward. The pursuer has to catch up 10 additional kilometers in the direction of the x axis, compared to the earlier setup where the players are separated only in the direction of the y axis. Consequently, the optimal direction of evasion changes considerably, being now almost aligned with the x axis. The control variable histories (not shown) are similar to the first case, except that because the pursuer is more aligned with the evader, the final transient in the bank angles does not appear. The identification takes 47.3 s.

Example 2: Intruder Flying Parallel to the Border

In the second example we consider a subsonic evader initially flying north, parallel to the borderline at $h_{E,0} = 5$ km. In this setting, the pursuer has the possibility to approach the evader also from behind to maximize its security (see Fig. 1c). We again assume that the pursuer approaches the evader with a high speed in a high altitude. A representative initial state z_0 corresponding to this engagement is

$$\begin{aligned} x_{P,0} &= 0\ \text{m}, & x_{E,0} &= 0\ \text{m} \\ y_{P,0} &= -10{,}000\ \text{m}, & y_{E,0} &= 0\ \text{m} \\ h_{P,0} &= 9000\ \text{m}, & h_{E,0} &= 5000\ \text{m} \\ v_{P,0} &= 550\ \text{m/s} = \text{Mach } 1.8, & v_{E,0} &= 200\ \text{m/s} = \text{Mach } 0.6 \\ \gamma_{P,0} &= 0\ \text{rad}, & \gamma_{E,0} &= 0\ \text{rad} \\ \chi_{P,0} &= \pi/2\ \text{rad}, & \chi_{E,0} &= \pi/2\ \text{rad} \end{aligned}$$

The optimal trajectories of both players are presented in Fig. 6. Here, the initial state is more favorable for the evader than in the earlier example because it does not have to turn and consume velocity as much. The evader is able to move 11.8 km eastward before becoming identified, and the encounter takes 40.0 s.

We compare the approach from behind to an approach from the side (see Fig. 1d). In this case approaching from the side places the pursuer 10 km farther west, which is clearly advantageous for the evader. The total displacement of the evader in the direction of the x axis, corresponding to the initial state

$$\begin{aligned} x_{P,0} &= -10{,}000\ \text{m}, & x_{E,0} &= 0\ \text{m} \\ y_{P,0} &= 0\ \text{m}, & y_{E,0} &= 0\ \text{m} \\ h_{P,0} &= 9000\ \text{m}, & h_{E,0} &= 5000\ \text{m} \\ v_{P,0} &= 550\ \text{m/s} = \text{Mach } 1.8, & v_{E,0} &= 200\ \text{m/s} = \text{Mach } 0.6 \\ \gamma_{P,0} &= 0\ \text{rad}, & \gamma_{E,0} &= 0\ \text{rad} \\ \chi_{P,0} &= 0\ \text{rad}, & \chi_{E,0} &= \pi/2\ \text{rad} \end{aligned}$$

amounts to 19.3 km, 63% more than in the approach from behind.

Finally, we determine an optimal direction of approach for the pursuer. The pursuer is allowed to select its initial coordinates $(x_{P,0}, y_{P,0})$ freely within a 10-km horizontal distance from the evader but it is required to stay west of the evader and to initially point towards it. The initial conditions corresponding to this setting are

$$\begin{aligned} x_{P,0}^2 + y_{P,0}^2 - D^2 &= 0, & x_{P,0} &< 0 \\ y_{P,0} &= 0\ \text{m}, & y_{E,0} &= 0\ \text{m} \\ h_{P,0} &= 9000\ \text{m}, & h_{E,0} &= 5000\ \text{m} \\ v_{P,0} &= 550\ \text{m/s} = \text{Mach } 1.8, & v_{E,0} &= 200\ \text{m/s} = \text{Mach } 0.6 \\ \gamma_{P,0} &= 0\ \text{rad}, & \gamma_{E,0} &= 0\ \text{rad} \\ \chi_{P,0} &= \arctan(y_{P,0}/x_{P,0})\ \text{rad}, & \chi_{E,0} &= \pi/2\ \text{rad} \end{aligned}$$

where $D = 10{,}000$ m. For this initial direction of the evader, the most advantageous direction of approach turns out to be from the front. The direction forces the evader to make a sharp turn, which just consumes the evader's velocity without considerably increasing the x coordinate. The outcome of the game is 9.92 km. The final time is 34.7 s. Note, however, that in reality, pilots are perhaps not willing to face an unknown target from the front.

Comments on the Solutions

The dynamic pressure constraint of the evader becomes active in every case. It prevents the evader from diving steeply and shortens the distance the evader can move. Note that despite the constraint, the initial velocity difference of the players greatly affects the outcome of the game. For example, if in the first case of example 2 the evader's initial velocity were 400 m/s, the outcome would be more than 40 km and the final time approximately 90 s.

The dynamic pressure constraint of the pursuer remains inactive. A smaller limit would cut down the pursuer's velocity, which would prolong the game and benefit the evader. Values of $q_{P,\max}$ close to $q_{E,\max}$ would probably lead to very long final times and large payoffs because the pursuer could then catch up the evader only very slowly. The minimum altitude constraints remain inactive in every case.

The pursuer stays behind the evader in every example. A solution where the pursuer would fly in front of the evader during the encounter would be rather problematic because in practice the pursuer should avoid drifting to the front sector of the evader. The evader also decelerates in the end of every example to delay the capture. The extra range gained by the deceleration depends to some extent on $n_{\max}$ and the weighting factor κ, cf. Eqs. (18) and (48). For reasonable values of the parameters, the increase in these examples is some percents compared to the case where the evader is not equipped with an airbrake. In practice, it is questionable whether the evader would implement the optimal deceleration because the increase in the payoff is obtained at the expense of a considerable velocity loss that is often avoided by all possible means.

At the termination, the pursuer is approximately 100 m behind the evader, with an approximately 20 m/s larger velocity. This should provide at least 5 s for the pursuer to correct the remaining deviation in the heading angle, which is typically at most 20 deg. The final flight-path angles are practically equal. A detailed investigation of the final conditions would require a separate analysis.

The numerical method converged in about 10 iterations in a particular example, that is, some 20 optimization problems were solved in each case. As an example, the evolution of the payoff in the last case of example 2 is shown in Fig. 7. The initial estimate of the evader's trajectory is a loose turn toward the border in the horizontal plane. Overall, the method is rather insensitive with regard to the initial estimate; only a rough idea of the evader's nominal trajectory is required. Another estimate is needed to initiate the computation of the pursuer's minimization problem. This estimate does not have to be feasible. No adjoint variables, different jump parameters, or the switching structure of the solution need to be specified in advance. In the iteration, previous solutions of the optimization problems are used as the initial estimate for the next problems. Because the previous solution very likely lies in the convergence domain of the next problem, convergence of individual optimization problems is highly satisfactory.

The total computing time of a particular solution with a Compaq Alphaserver SG140 type mainframe of the Finnish Center for Scientific Computing were typically some minutes. If a more accurate solution is needed, the solutions obtained here, together with the corresponding Lagrange multipliers, can be used as initial estimates for the state and adjoint trajectories in an indirect solution method, cf. Ref. 18.

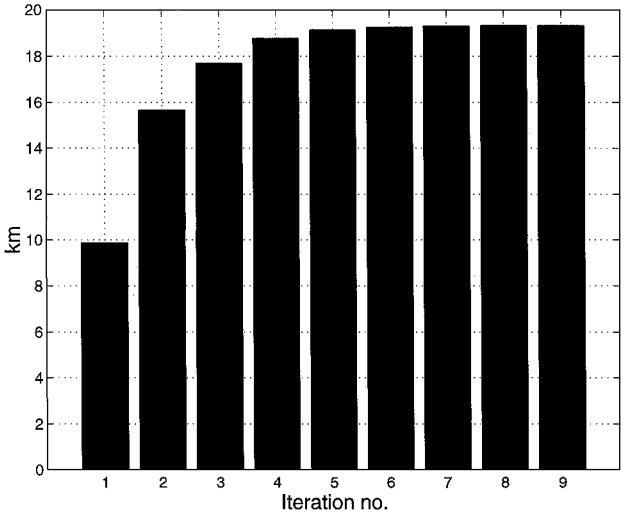

Fig. 7 Evolution of the payoff in the second case of example 2.

Conclusions

We have studied optimal behavior of two aircraft, an intruder and an identifier, in a situation where the identifier wants to capture the intruder before it crosses a state border. The atmosphere and the aerodynamic properties as well as the thrust of both aircraft are modeled using realistic data. Along optimal trajectories both players decelerate in the end, which is taken into account in the modeling to prevent chattering controls.

The complexity of the setting prevents a comprehensive analysis, but approximate open-loop representations of feedback strategies can be computed with the presented solution method. The method decomposes the necessary conditions into two optimal control problems that are solved in turns using discretization and nonlinear programming until the solution is reached.

Based on the numerical examples it seems that the evader chooses its direction of evasion as a compromise between x range and y range and that this direction is away from the pursuer. There may exist solutions in which it is optimal for the evader to turn against the pursuer, but they seem to correspond to unrealistic initial constellations where the pursuer would be slow and very close to the evader.

The game model can be used to estimate the largest possible displacement of the evader toward the border in different scenarios. This provides an estimate for the success of the identification: If the predicted displacement is smaller than the evader's current distance to the border, the identification will be successful, provided that optimal actions are taken by the pursuer. Thus, the model helps not only in determining the optimal identification strategy but also in allocating the identifiers and in planning the identification flight.

What we have not modeled here is the possible dependence of the initial separation of the players on the pursuer's direction of approach. It may be that the pursuer can initially approach the evader much closer from behind than from the front, for example. This of course depends on the capability of the evader to notice the pursuer. In any case, it seems favorable for the pursuer to approach the evader from such an initial position that maximizes the pursuer's initial x coordinate.

Acknowledgment

This work has been carried out in collaboration with the Finnish Air Force.

References

[1]Petrosjan, L., *Differential Games of Pursuit*, World Scientific Publishing, Singapore, Republic of Singapore, 1993, p. 51.

[2]Järmark, B., and Bengtsson, H., "Near Optimal Flight Trajectories Generated by Neural Networks," *Computational Optimal Control*, edited by R. Bulirsch and D. Kraft, Birkhäuser, Basel, Switzerland, 1993, pp. 319–328.

[3]Seywald, H., "Trajectory Optimization Based on Differential Inclusion," *Journal of Guidance, Control, and Dynamics,* Vol. 17, No. 3, 1994, pp. 480–487.

[4]Lachner, R., Breitner, M., and Pesch, H., "Efficient Numerical Solution of Differential Games with Application to Air Combat," Rept. 466, Inst. of Mathematics, Technical Univ. of Munich, Munich, 1993.

[5]Raivio, T., and Ehtamo, H., "On the Numerical Solution of a Class of Pursuit–Evasion Games," *Annals of the International Society on Dynamic Games and Applications* (to be published).

[6]Ehtamo, H., and Raivio, T., "Applying Nonlinear Programming to Pursuit–Evasion Games," Helsinki Univ. of Technology, Systems Analysis Lab. Research Rept. E4, March 2000.

[7]Hargraves, C. R., and Paris, S. W., "Direct Trajectory Optimization Using Nonlinear Programming and Collocation," *Journal of Guidance, Control, and Dynamics*, Vol. 10, No. 4, 1987, pp. 338–342.

[8]von Stryk, O., and Bulirsch, R., "Direct and Indirect Methods for Trajectory Optimization," *Annals of Operations Research*, Vol. 37, 1992, pp. 357–373.

[9]Raivio, T., Ehtamo, H., and Hämäläinen, R. P., "Aircraft Trajectory Optimization Using Nonlinear Programming," *System Modeling and Optimization*, edited by J. Dolezal and J. Fidler, Chapman and Hall, London, 1996, pp. 435–441.

[10]Betts, J., "Survey of Numerical Methods for Trajectory Optimization," *Journal of Guidance, Control, and Dynamics*, Vol. 21, No. 2, 1998, pp. 193–207.

[11]Basar, T., and Olsder, G., *Dynamic Noncooperative Game Theory,* 2nd

ed., Academic Press, London, 1995, pp. 254, 451, 452.

[12]Seywald, H., "Range Optimal Trajectories for an Aircraft Flying in the Vertical Plane," *Journal of Guidance, Control, and Dynamics,* Vol. 17, No. 2, 1994, pp. 389–398.

[13]Miele, A., *Flight Mechanics*, Addison–Wesley, Reading, MA, 1962.

[14]Isaacs, R., *Differential Games,* Krieger, New York, 1975, pp. 132–155, 202, 273, reprint.

[15]Breitner, M., Pesch, H., and Grimm, W., "Complex Differential Games of Pursuit–Evasion Type with State Constraints, Part II: Multiple Shooting and Homotopy," *Journal of Optimization Theory and Applications*, Vol. 78, No. 3, 1993, pp. 442–464.

[16]Shimitsu, K., Ishizuka, Y., and Bard, J., *Nondifferentiable and Two-Level Mathematical Programming,* Kluwer, Boston, 1997.

[17]Gill, P., Murray, W., Saunders, M., and Wright, M., "User's Guide for NPSOL 4.0: A Fortran Package for Nonlinear Programming," Rept. SOL 86-4, Stanford Univ., Stanford, CA, 1986.

[18]Lachner, R., Breitner, M., and Pesch, H. J., "Three-Dimensional Air Combat: Numerical Solution of Complex Differential Games," *New Trends in Dynamic Games and Applications*, edited by G. J. Olsder, Birkhäuser, Boston, 1996, pp. 165–190.